Observations of a Severe, Left-Moving Supercell on 4 May 2003

DANIEL T. LINDSEY*

Cooperative Institute for Research in the Atmosphere, Fort Collins, Colorado

MATTHEW J. BUNKERS

NOAA/National Weather Service Forecast Office, Rapid City, South Dakota

(Manuscript received 30 January 2004, in final form 7 July 2004)

ABSTRACT

A case study of a left-moving supercell with a rapid motion is presented to (i) elucidate differences in anvil orientations between left- and right-moving supercells and (ii) highlight the interaction of the left mover with a tornadic right mover. It is shown how anvil orientations, as viewed from satellite, may be used to assist in the identification of thunderstorms with differing motions and how this applies to splitting supercells. Additionally, the movement of the left mover into the forward flank of the right mover may have temporarily affected its tornadic circulation, as tornadoes occurred both before and after the merger, despite the structure of the right mover being interrupted during the merging process. Given the dearth of literature on thunderstorm mergers in general, and how mergers affect tornadic supercells in particular, this is an area that demands further research.

1. Introduction

Documentation of left-moving supercell thunderstorms has been relatively rare in the literature (Dostalek et al. 2004). Considerable attention has been given to right-moving supercells, primarily because they are much more common in the United States than their left-moving counterparts (Davies-Jones 1986; Bunkers 2002). Numerical modeling results in the early 1980s indicate symmetric splitting supercells can occur in a unidirectionally sheared environment. The left mover (right mover) is favored when the low-level shear vector turns counterclockwise (clockwise) with height (Weisman and Klemp 1984, 1986). A few observational studies of left-moving supercells support these findings (e.g., Nielsen-Gammon and Read 1995; Grasso and Hilgendorf 2001). Here we present a case study of a severe, left-moving supercell from 4 May 2003 that affected northeastern Oklahoma and extreme southwestern Missouri. Noteworthy aspects of this case study include (i) the storm's rapid motion and associated anvil orientation with respect to that of the right mover, and (ii) interaction/merger of the left mover with a tornadic right-moving supercell, which may have affected its tornadic circulation.

2. Case study

a. Synoptic setup

The storm of interest occurred in a large-scale environment that was favorable for severe storms. There was a deep trough over the western United States and a strong southerly flow of moist and unstable air at low levels across the southern and central plains. This day marked the beginning of an 8-day period of numerous tornado reports over the central plains and mid–Mississippi River valley (NOAA 2004). A special sounding at Norman, Oklahoma (1800 UTC 4 May 2003; Fig. 1), and the routine sounding at Springfield, Missouri (0000 UTC 5 May 2003), indicated the MLCAPE was 2346 J kg^{-1} and 2143 J kg^{-1}, respectively (MLCAPE is herein defined as the CAPE computed by mixing the lowest 1000 m of the environment, then lifting a parcel from this layer). Midlevel dry air capped a warm and moist boundary layer near 800 hPa (Fig. 1); however, convective inhibition was still less than 15–25 J kg^{-1}. This instability, combined with 0–6-km AGL bulk shear of 35 m s^{-1} (70 kt), suggested the environment was highly conducive to supercells (e.g., Rasmussen and Blanchard 1998). Indeed, thunderstorms developed rapidly along a surface convergence line in northeastern Kansas by 1900 UTC (Fig. 2), many of which

* Current affiliation: NOAA/NESDIS/ORA, Fort Collins, Colorado.

Corresponding author address: Daniel T. Lindsey, Cooperative Institute for Research in the Atmosphere—1375 Campus Delivery, Colorado State University, Fort Collins, CO 80523.
E-mail: lindsey@cira.colostate.edu

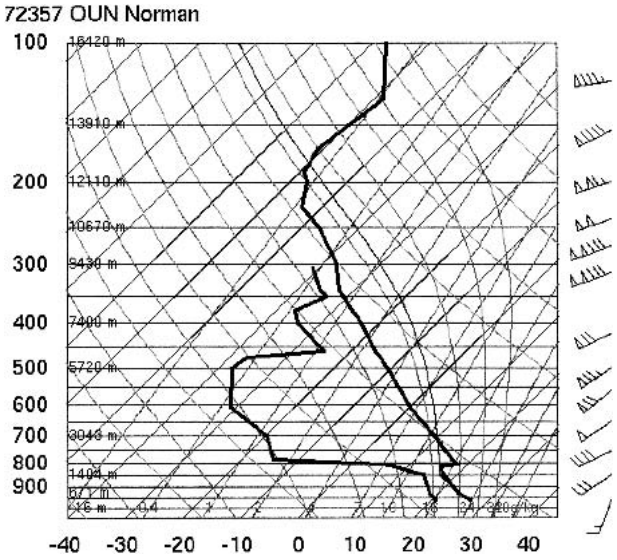

FIG. 1. Sounding from Norman, OK, at 1800 UTC 4 May 2003 (courtesy of the University of Wyoming).

eventually developed supercellular characteristics. A dryline—characterized by a 17°C (30°F) dewpoint temperature difference—was located west of this convergence line, extending from northeastern Kansas southwestward into west-central Oklahoma.

b. Supercell evolution

An area of thunderstorms initiated in southeastern Oklahoma on the southern end of a convergence line shortly after 2000 UTC, with storm splitting occurring between 2041 and 2111 UTC per the Weather Surveillance Radar-1988 Doppler (WSR-88D) at Tulsa, Oklahoma (KINX; see Fig. 9 for location); *Geostationary Operational Environmental Satellite-12* (*GOES-12*) imagery were also able to depict the split between 2045 and 2145 UTC (Fig. 3). The right-moving[1] supercell in southeastern Oklahoma progressed east-northeastward and took on a classic supercellular appearance (as viewed from the KINX radar; not shown), while the left mover tracked rapidly northeastward. A second group of thunderstorms formed along the dryline in northeastern Oklahoma around 2030 UTC, and another right-moving supercell progressed east-northeastward toward the northeastern corner of Oklahoma (Figs. 3a–f; also see Fig. 8). By 2302 UTC, the rapidly moving left-moving supercell was about to collide with the tornadic right mover in extreme northeastern Oklahoma; this interaction will be discussed in section 2d. Using radar data from KINX, the left-moving supercell's motion was 219° at 34 m s^{-1} (66 kt) from 2100 to 2300 UTC, while the motion of the right-moving supercell in extreme northeastern Oklahoma was 256° at 21 m s^{-1} (40 kt).

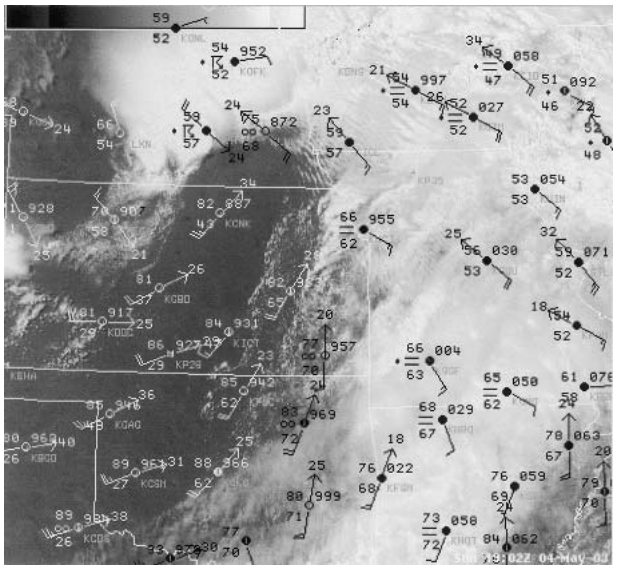

FIG. 2. *GOES-12* visible satellite image (1902 UTC 4 May 2003) overlaid with surface observations (1900 UTC 4 May 2003).

Severe weather was reported with all three supercells discussed above (NCDC 2003), with both right movers producing tornadoes. The right mover in southeastern Oklahoma produced large hail [7.0-cm (2.75 in.) diameter was the largest report], damaging wind [28 m s^{-1} (54 kt) was the highest gust], and an F0 tornado. The right mover in northeastern Oklahoma and far southwestern Missouri produced large hail [10.8-cm (4.25 in.) diameter was the largest report] and F2–F3 tornadoes. The left mover produced large hail [7.0-cm (2.75 in.) diameter was the largest report] and damaging wind [36 m s^{-1} (70 kt) was the highest gust]. The higher wind gusts with the left mover, relative to the right mover, are consistent with its faster motion [i.e., the left mover moved 13 m s^{-1} (26 kt) faster than the right mover].

Figure 4 is a hodograph from the wind profiler in Haskell, Oklahoma (see Fig. 9 for location), about 1 h before the left mover passed within a few miles of the profiler location. To a first-order approximation the hodograph is a straight line from the surface to 3 km, which engenders splitting supercells. Positive values of storm-relative helicity (SRH) for the right mover and negative values of SRH for the left mover are favorable for the maintenance of both storm types (Davies-Jones et al. 2001). However, there are some important, yet subtle, hodograph curvature characteristics in the lowest levels. First, the surface–2-km hodograph curves in a clockwise direction, while the hodograph in the 2–4-km layer exhibits counterclockwise curvature. This low-level clockwise curvature is favorable for tornadogenesis in the right mover, but unfavorable for the left mover since positive streamwise vorticity would enter

[1] Storm-relative velocity (SRM) data were used to verify the existence of cyclonic (anticyclonic) rotation within the right-moving (left moving) supercells discussed in the text.

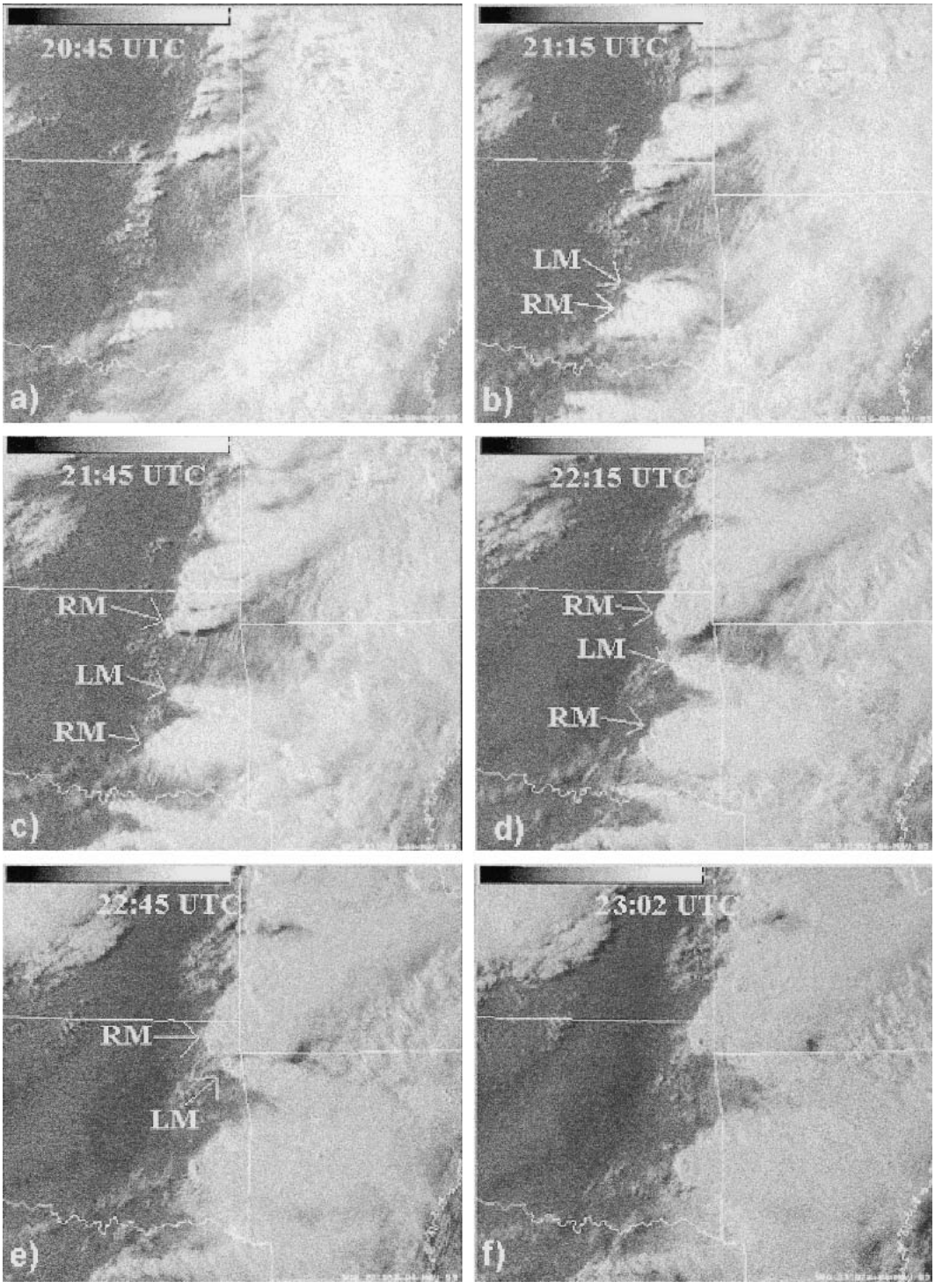

FIG. 3. *GOES-12* visible satellite progression at (a) 2045, (b) 2115, (c) 2145, (d) 2215, (e) 2245, and (f) 2302 UTC 4 May 2003. Here, LM and RM point toward the left-moving and right-moving storms discussed in the text.

the left mover's updraft near the surface (Davies-Jones et al. 2001). Accordingly, the 0–1-km SRH was 157 m^2 s^{-2} (-46 m^2 s^{-2}) given the observed motion of the tornadic right-moving (nontornadic left moving) supercell. Thompson et al. (2003) found that similar values of positive 0–1-km SRH are favorable for supercells producing significant tornadoes. Finally, the counterclockwise curvature from 2 to 4 km apparently was not a detrimental factor to the sustenance of right-moving supercells. However, this "reverse S shaped" hodo-

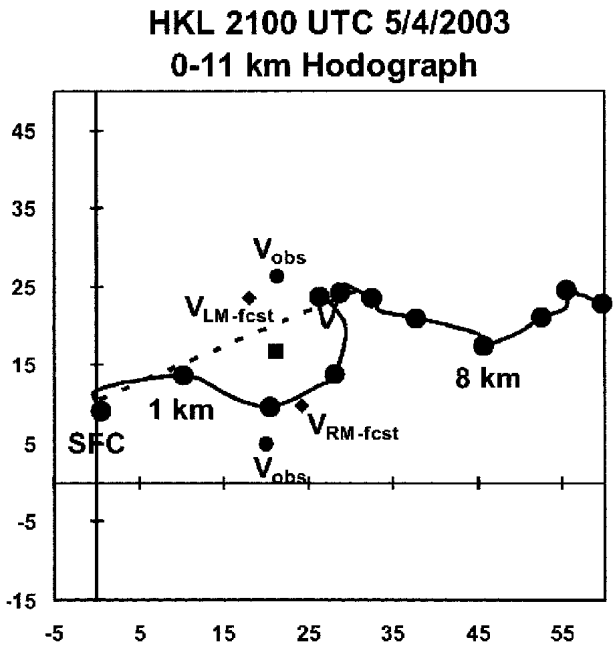

FIG. 4. Hodograph derived from the Haskell, OK, wind profiler valid at 2100 UTC 4 May 2003. Data are plotted every 500 m AGL, and filled circles are at every 1 km AGL (m s^{-1}). The observed storm motions are plotted for the left- (V_{obs}) and right-moving (V_{obs}) supercells in northeastern OK; the forecast supercell motions are plotted for the left- ($V_{LM\text{-}fcst}$) and right-moving ($V_{RM\text{-}fcst}$) supercells using the method of Bunkers et al. (2000); the 0–6-km mean wind is indicated with a filled square; and the shear from the boundary layer to 6 km is represented with a dashed line.

graph configuration still demands further investigation because it has not been adequately addressed in modeling studies, and it may be important from a forecasting perspective.

Bunkers et al. (2000) developed a simple empirical technique to predict supercell motion based on the vertical wind shear profile (i.e., the hodograph). Their primary assumption is that supercell motion is the vector sum of (i) advection via a representative mean wind vector and (ii) shear-induced propagation to the left (right) of the vertical wind shear vector for a left-moving (right moving) supercell. For hodographs in the upper-right quadrant, as in the present case (Fig. 4), this often leads to a left-moving supercell that moves faster than the mean wind through the lowest 6 km, and a right mover that moves slower than the mean wind. Therefore, the existence of the hodograph in the northeastern quadrant helps explain the rapid motion of the left-moving supercell, relative to the right mover {as well as to the mean wind [i.e., the arithmetically averaged 0–6-km mean wind was 232° at 27 m s^{-1} (52 kt)]}.

c. Anvil orientation

An interesting feature observed from satellite imagery was the difference in the orientation of the anvils of the left and right movers—a direct result of the disparate storm motions. Fujita and Grandoso (1968) first documented the difference in anvil orientations between a cyclonic and anticyclonic rotating storm pair using radar data. Similarly, using satellite data, we note the anvil of the left mover was oriented in a west-northwest to east-southeast direction, while the anvil of the right mover was oriented southwest to northeast (Fig. 5; also see Fig. 3)—resulting in about a 50° difference between the anvils for the left and right movers. Anvil motion depends not only on the anvil-level winds, but also on the motion of the storm itself, which explains the large difference in anvil orientation. Anvil orientation is the direction of the vector difference between the anvil-level wind vector and the storm motion vector. Graphically, this vector would point from V_{obs} to the anvil-level wind (Fig. 4). However, as noted by Fujita and Grandoso (1968), the anvil is steered by winds throughout an upper-level layer, and not just by the wind at one specific level. In the present case, the vector from V_{obs} (for the left mover) to the 8-km wind appears to best match the anvil orientation of the left mover from the GOES visible satellite—relative to the 9–11-km winds (cf. Figs. 4 and 5)—even though the anvil top was located above 11 km. So perhaps choosing a single upper level is reasonable to a first-order approximation. Two storms that are sufficiently close together will experience the same anvil-level winds, allowing inferences to be made about their storm motions based on the orientation of their anvils. This observation suggests that two storms moving in different directions (e.g., left- and right-moving supercells) can be identified with satellite data using only the orientation of the anvils (when there are no intervening clouds).

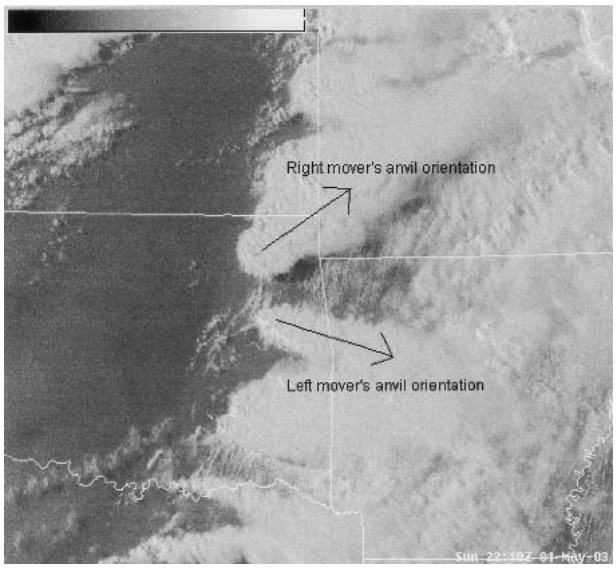

FIG. 5. *GOES-12* visible satellite at 2110 UTC 4 May 2003. Anvil orientations of the left and right movers are designated by arrows.

In order to better understand the range of differences between the anvil orientations of left- and right-moving supercells, the hodographs and observed storm motion vectors for 479 right-moving supercells from Bunkers (2002) were used to construct a distribution of "anvil orientations." First, the observed storm motions for the 479 right-moving supercells, along with the 8-km wind [taken as a proxy of the anvil-level wind based on Fig. 4 as well as Fujita and Grandoso (1968)], were used to calculate the anvil orientations for the right movers. For comparison purposes, the same dataset was used to estimate the hypothesized left-moving supercell motion [using the empirical formula from Bunkers et al. (2000)] since there were no observed motions. The anvil orientations were then derived for this hypothetical distribution of left-moving supercells.

Based on this dataset and methodology, 92% of the cases exhibited differences in anvil orientation between +10° and +90°, where the plus sign indicates that the anvil orientation of the left mover was farther to the right (in a clockwise sense) than that of the right mover (Fig. 6). The mean absolute value of the differences was 58° and the median difference was 54°. The present case is rather typical when put in this perspective (e.g., refer back to Fig. 5). Also of interest, only 3% of the cases (12 of 479) had orientations where the anvil of the right mover was to the right of the left mover (negative values in Fig. 6). Since anvil orientations are Galilean invariant, these cases are not the result of "atypical" hodograph orientations. Instead, these were cases where either (i) the anvil-level winds folded back onto themselves (Fig. 7a; 8 of the 12 cases), or (ii) the observed right-moving supercell motion was faster than the winds throughout the lowest 8 km (Fig. 7b; 4 of the 12 cases). In the first situation, the anvil orientation would be similar using both the observed and predicted motion of the right mover (Fig. 7a; 30° difference). However, the anvil orientation would be about 180° out of phase in the second situation depending upon whether the observed or forecast storm motion was used (Fig. 7b). Given the scenario in Fig. 7b where storm motion was beyond the hodograph, it is possible that these cases represent 1) heavy precipitation (HP) supercells that were outflow dominated or 2) supercells that were

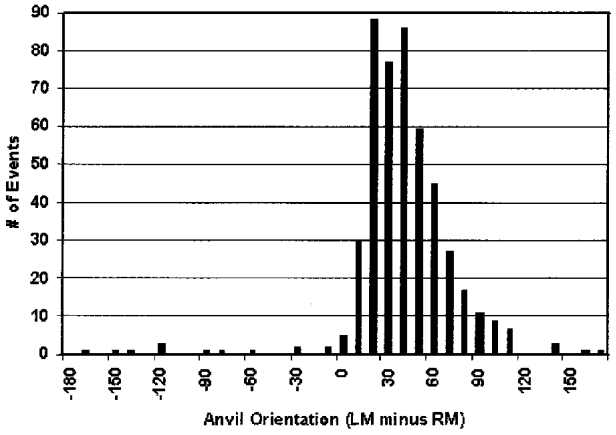

FIG. 6. Distribution of differences in anvil orientation direction between left- and right-moving supercells. Positive values denote the anvil orientation direction was rotated clockwise for the left mover relative to the right mover.

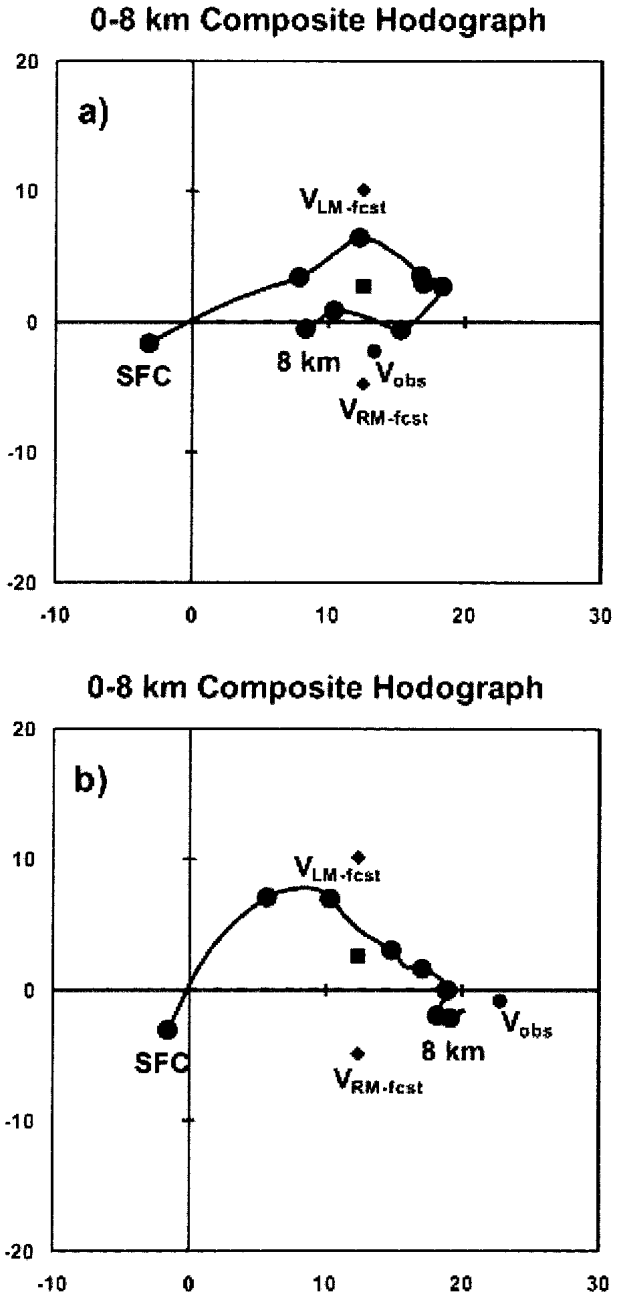

FIG. 7. Same as in Fig. 4 except for (a) composite hodograph derived from eight cases where "reverse" shear was present at anvil level and (b) composite hodograph derived from four cases where the observed storm motion was faster than any of the winds in the lowest 8 km. The compositing procedure is the same as in Bunkers (2002).

associated with bow echoes. Since the median difference in anvil orientations between left and right movers is approximately 54°, this satellite technique of identifying storms with disparate motions is feasible.

d. Storm interaction

Figure 8 is a six-panel radar progression from the WSR-88D radar at Springfield, Missouri (KSGF), showing the left mover's interaction with the right mover in extreme northeastern Oklahoma and southwestern Missouri. An F1 tornado was reported with the right mover in Ottawa County, Oklahoma, around 2300 UTC (near the time in Fig. 8a; tornado location denoted by T), prior to the merger. The left mover had completely intersected the forward flank of the right mover by 2317 UTC (Fig. 8c), before weakening as it continued to the northeast (Figs. 8d–f). During and immediately following the merger, there were no tornado reports. Additionally, the right mover's hook-echo appendage became ill defined as it crossed into Missouri, then regained its identity by 2347 UTC (Fig. 8f). There were no more tornado reports until 2340 UTC, when the storm was producing an F2 tornado in eastern New-

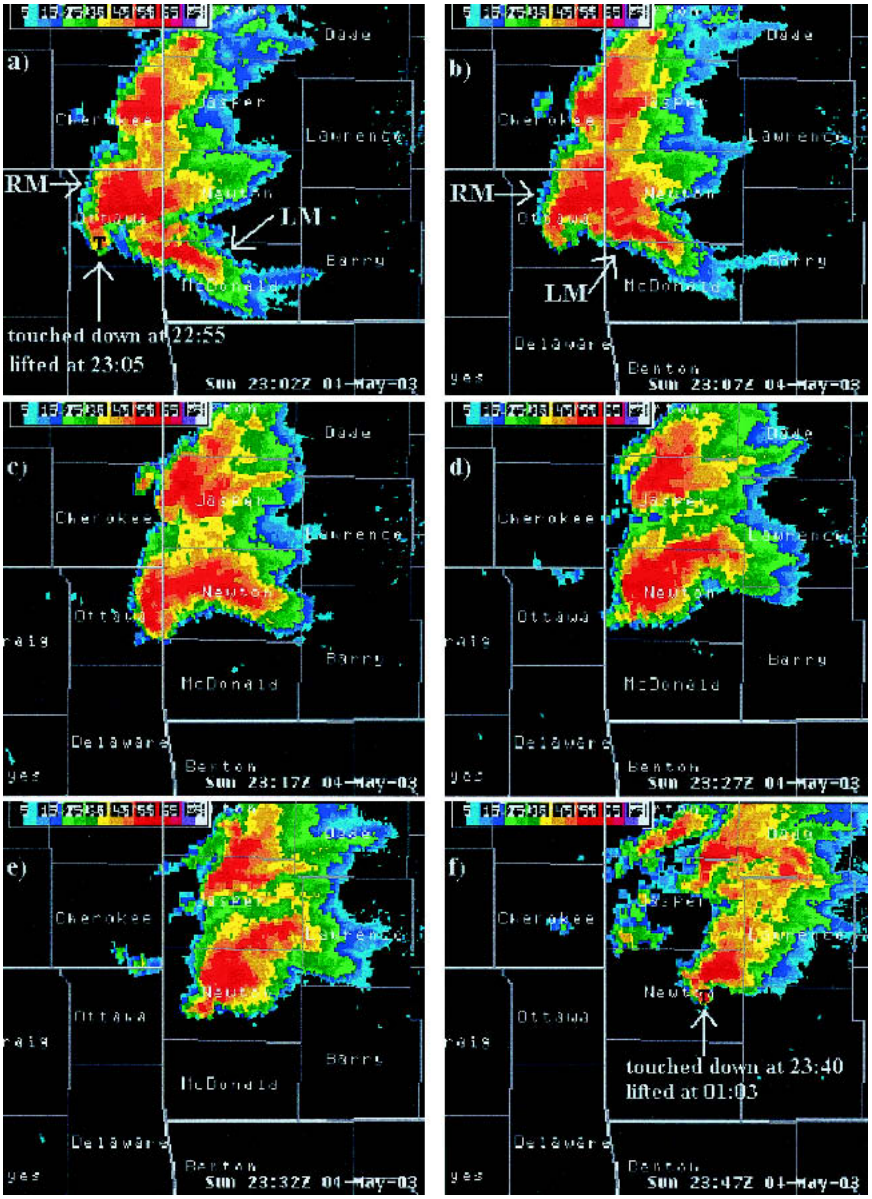

FIG. 8. A 0.5° tilt base reflectivity from the KSGF WSR-88D radar valid at (a) 2302, (b) 2307, (c) 2317, (d) 2327, (e) 2332, and (f) 2347 UTC. Right mover (left mover) designated by RM (LM). Location of observed tornado indicated with a T in (a) and (f).

ton County (Fig. 8f; tornado location denoted by T), and eventually an F3 tornado in Lawrence County. This suggests that the left mover may have temporarily disrupted the tornadic circulation of the right mover, perhaps by affecting its inflow. From 2302 to 2317 UTC, the left mover was producing precipitation in northern McDonald and southern Newton Counties (Figs. 8a–c); this is the precise area from which the right mover's inflow originated as it crossed the state border into Missouri.

Both Springfield and Tulsa radars were able to estimate the height of the storm's echo top. At 2305 UTC, just before the interaction, the right-mover's overshooting top extended to 17–20 km above mean sea level (MSL). By 2315 UTC, the top had decreased to 15.5–18 km MSL, and at 2330 UTC, the highest echo was located 13–16 km MSL. After the interaction, the echo top began increasing again; by 2341 UTC, it was located 16.5–19 km MSL, indicating a very strong updraft had again developed. These data suggest that the right-mover's updraft weakened during its interaction with the left mover.

There was at least one other left-moving supercell on this day [moving from 217° at 27 m s^{-1} (53 kt)], and it also intersected, and merged with, an adjacent right-moving supercell in southeastern Kansas. In order to put the present case into better perspective, the occurrence of tornadoes centered around this interaction was also investigated. An F1 tornado was initially reported with the right-moving supercell at 2206 UTC, just prior to the merger with the left mover. The tornado persisted until 2225 UTC, at which time both storms had completely merged near the Missouri border. The right mover subsequently become disorganized and ceased producing tornadoes. The storm then reorganized about 30 min after the merger, and produced an F2 tornado from 2304 to 2353 UTC in west-central Missouri. Therefore, this case is similar to the one discussed above in that the supercell was tornadic just prior to the merger, became disorganized during and immediately following the merger, but then reintensified to produce additional strong tornadoes. It is unknown if the two left movers played any role in the reintensification of these tornadic right movers, or if they just temporarily

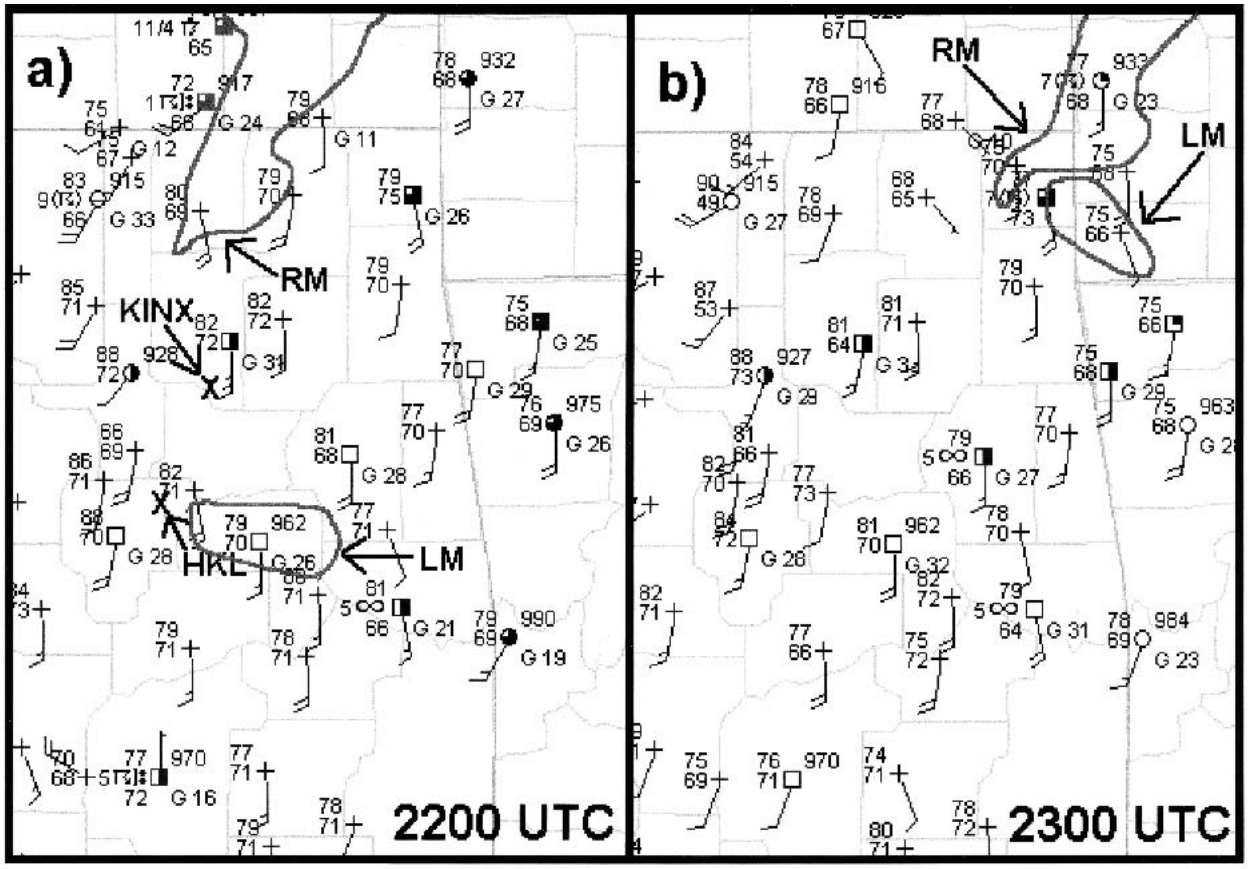

FIG. 9. Surface station plots from the Oklahoma mesonet at (a) 2200 and (b) 2300 UTC. Northeast OK, northwest AR, southeast KS, and southwest MO, are shown. KINX and HKL show the locations of the Tulsa radar and the Haskell wind profiler, respectively. Dark gray contours show the approximate location of the 25-dBZ 0.5° tilt radar contour from KINX for RM and LM in northeast OK which interact shortly after 2300 UTC.

interrupted an otherwise persistent storm. It is worth noting that both tornadic storms produced long-track tornadoes after the merger.

3. Summary and conclusions

A left-moving supercell in northeastern Oklahoma on 4 May 2003 was analyzed with respect to its evolution, anvil orientation, and interaction with another tornadic right-moving supercell. It moved 13 m s^{-1} (26 kt) faster than its right-moving counterpart and produced very large hail, but no tornadoes. The differential motion of these supercells resulted in unique anvil orientations, which were readily apparent in *GOES-12* visible satellite images. This case highlights the potential usefulness of satellite imagery in inferring differential motion between supercells.

Furthermore, as the left mover interacted with a tornadic right-moving supercell, it seemingly disrupted its rotation, suggesting the merger had a disorganizing effect on the right mover. Several studies have discussed—or briefly mentioned—the effects of storm mergers on tornadogenesis (e.g., Stout and Hiser 1955; Bluestein and Parker 1993; Finley et al. 2001; Dowell and Bluestein 2002), but few have focused specifically on left-mover–right-mover mergers.

Since the left mover progressed through the inflow portion of the right mover, it likely altered both the thermodynamics of the inflow and the ambient wind field into which the right mover progressed. The left mover intersected the forward flank of the right mover, so the anticyclonic rotating updraft of the left mover may have destructively interfered with the cyclonic rotating updraft of the right mover, resulting in less net rotation and therefore storm disorganization. In addition, Oklahoma mesonet data (Figs. 9a,b) show that the temperature and dewpoint dropped by approximately 1°–2°C in the wake of the left mover, which is consistent with the detailed analyses of Charba and Sasaki (1971, their Fig. 6). The inflow air for the right mover would therefore be slightly more stable than the ambient air, which could slightly weaken the right-mover's updraft. Since this study presents a single example, and little additional information is present in the published literature, mergers between right- and left-moving supercells and the resulting effects on tornadogenesis are topics that deserve further study.

Acknowledgments. This research presented in this study was supported by NOAA Grant NA17RJ1228. We would like to thank Drs. Mark DeMaria, Andy Detwiler, Paul Smith, and Jim Purdom, as well as John Weaver, Jack Dostalek, and Jon Zeitler, for reviewing this manuscript and providing excellent suggestions for improvement. Additionally, very insightful comments from three anonymous reviewers significantly improved this manuscript.

REFERENCES

Bluestein, H. B., and S. S. Parker, 1993: Modes of isolated, severe convective storm formation along the dryline. *Mon. Wea. Rev.,* **121,** 1354–1372.

Bunkers, M. J., 2002: Vertical wind shear associated with left-moving supercells. *Wea. Forecasting,* **17,** 845–855.

——, B. A. Klimowski, J. W. Zeitler, R. L. Thompson, and M. L. Weisman, 2000: Predicting supercell motion using a new hodograph technique. *Wea. Forecasting,* **15,** 61–79.

Charba, J., and Y. Sasaki, 1971: Structure and movement of the severe thunderstorms of 3 April 1964 as revealed from radar and surface mesonetwork data analysis. *J. Meteor. Soc. Japan,* **49,** 191–213.

Davies-Jones, R. P., 1986: Tornado dynamics. *Thunderstorm Morphology and Dynamics,* E. Kessler, Ed., University of Oklahoma Press, 197–236.

——, R. J. Trapp, and H. B. Bluestein, 2001: Tornadoes and tornadic storms. *Severe Convective Storms, Meteor. Monogr.,* No. 50, Amer. Meteor. Soc., 167–221.

Dostalek, J. F., J. F. Weaver, and G. L. Phillips, 2004: Aspects of a tornadic left-moving thunderstorm of 25 May 1999. *Wea. Forecasting,* **19,** 614–626.

Dowell, D. C., and H. B. Bluestein, 2002: The 8 June 1995 McLean, Texas, storm. Part I: Observations of cyclic tornadogenesis. *Mon. Wea. Rev.,* **130,** 2626–2648.

Finley, C. A., W. R. Cotton, and R. A. Pielke Sr., 2001: Numerical simulation of tornadogenesis in a high-precipitation supercell. Part I: Storm evolution and transition into a bow echo. *J. Atmos. Sci.,* **58,** 1597–1629.

Fujita, T., and H. Grandoso, 1968: Split of a thunderstorm into anticyclonic and cyclonic storms and their motion as determined from numerical model experiments. *J. Atmos. Sci.,* **25,** 416–439.

Grasso, L. D., and E. R. Hilgendorf, 2001: Observations of a severe left-moving thunderstorm. *Wea. Forecasting,* **16,** 500–511.

NCDC, 2003: *Storm Data.* Vol. 45, No. 5, 462 pp. [Available from National Climatic Data Center, 151 Patton Ave., Asheville, NC 28801-5001.]

Nielsen-Gammon, J. W., and W. L. Read, 1995: Detection and interpretation of left-moving severe thunderstorms using the WSR-88D: A case study. *Wea. Forecasting,* **10,** 127–140.

NOAA, cited 2004: Record tornado outbreaks of May 4–10, 2003. Dept. of Commerce, NOAA/NWS Service Assessment. [Available online at http://www.nws.noaa.gov/om/assessments/record-may.pdf.]

Rasmussen, E. N., and D. O. Blanchard, 1998: A baseline climatology of sounding-derived supercell and tornado forecast parameters. *Wea. Forecasting,* **13,** 1148–1164.

Stout, G. E., and H. W. Hiser, 1955: Radarscope interpretations of wind, hail, and heavy rainstorms between May 27 and June 8, 1964. *Bull. Amer. Meteor. Soc.,* **36,** 519–527.

Thompson, R. L., R. Edwards, J. A. Hart, K. L. Elmore, and P. Markowski, 2003: Close proximity soundings within supercell environments obtained from the Rapid Update Cycle. *Wea. Forecasting,* **18,** 1243–1261.

Weisman, M. L., and J. B. Klemp, 1984: The structure and classification of numerically simulated convective storms in directionally varying wind shears. *Mon. Wea. Rev.,* **112,** 2479–2498.

——, and ——, 1986: Characteristics of isolated convective storms. *Mesoscale Meteorology and Forecasting,* P. S. Ray, Ed., Amer. Meteor. Soc., 331–358.